Design and Experimental Validation of a Noninvasive Glucose Monitoring System Using RF Antenna-Based Biosensor

Yaqub Mahnashi, *Senior Member, IEEE*, Khurram Karim Qureshi, *Senior Member, IEEE*, Abdullah A. Al-Shehri, and Hussein Attia, *Member, IEEE*

***Abstract*—This article presents an end-to-end microwave-based system to detect the glucose level in aqueous solutions through a noninvasive scheme. A microwave signal is generated and transmitted through the sample under test (i.e., glucose–water solution). The received signal is then conditioned using a low-noise amplifier (LNA), a bandpass filter (BPF), and an RF detector. The change in the dc output voltage on the receiver side is used as a new way to detect the glucose level. The proposed glucose sensor is implemented using two RF microstrip patch antennas that resonate at 5.7 GHz and are fabricated using an FR-4 substrate. The design specifications of the sensing antennas are thoroughly studied and presented. The system is verified experimentally using glucose–water testing samples. The experimental results confirm the correlation between the glucose concentration and the dc output voltage for a concentration range of 0–5000 mg/dL. The effect of the transmitted power level on the system performance is also investigated. Finally, the proposed system is compared with the state-of-the-art systems reported in the literature.**

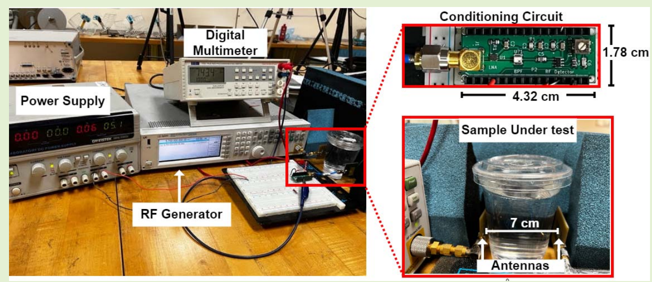

***Index Terms*—Biomedical applications, biosensors, glucose detection using RF sensors, noninvasive glucose monitoring.**

I. Introduction

THE widespread presence of diabetes in the last century has been highly associated with deleterious lifestyles, including unhealthy diet and limited physical activity. According to the World Health Organization (WHO), there had been a global increase to 8.5% in diabetes among adults in 2014 compared to 4.7% in 1980. About 1.6 million deaths were directly caused by diabetes in 2015 alone. Therefore, the diabetes medical management plan is essential to keep patients away from its complications, including cardiovascular disease, kidney damage, blindness, increased risk of stroke, and foot damage [1], [2].

Manuscript received 25 November 2022; accepted 3 December 2022. Date of publication 12 December 2022; date of current version 31 January 2023. This paper is based upon work supported by King Fahd University of Petroleum & Minerals (KFUPM). The authors acknowledge the KFUPM Interdisciplinary Research Center for Communication Systems and Sensing for the support received under Grant no. INCS2106. The associate editor coordinating the review of this article and approving it for publication was Prof. Yu-Cheng Lin. *(Corresponding author: Hussein Attia.)*

The authors are with the Electrical Engineering Department and the Center of Communication Systems and Sensing, King Fahd University of Petroleum and Minerals (KFUPM), Dhahran 31261, Saudi Arabia (e-mail: hattia@kfupm.edu.sa).

Digital Object Identifier 10.1109/JSEN.2022.3227382

Currently, most blood glucose monitoring systems rely on ambulatory devices that involve sampling the blood from a finger, using a lancet needle, to be analyzed [3]. However, in addition to being painful and causing high anxiety to the patients, these devices show high error rates in the range of 15% and up to 20% for old devices [4], [5]. Moreover, ambulatory devices perform capillary glucose measurement that is known to be inaccurate [3], [4]. Unfortunately, current ambulatory devices involve invasiveness, which is the main drawback that needs to be mitigated or eliminated to avoid harmful effects on patients. Furthermore, it is well known that commercially available devices for continuous blood glucose monitoring are costly and last for about two weeks only [6]. Therefore, a more reliable, low-cost, long-lasting, and efficient technology is needed to ensure continuous blood glucose monitoring without harming the patients psychologically or physically.

Recently, several noninvasive glucose-monitoring techniques have been considered. Examples include exhalation breath and biological body fluids analysis, in addition to many spectroscopic techniques that are unsuitable for continuous monitoring [7], [8], [9], [10], [11], [12]. Table I illustrates different noninvasive glucose-sensing techniques. However, these techniques exhibit notable drawbacks that may affect the

TABLE I
DIFFERENT GLUCOSE-SENSING TECHNIQUES

Technique	Description	Drawback
Raman spectroscopy [7], [8]	Uses laser light to measure the molecular vibration of the human fluids.	Unstable & suffers from high interference
Body fluids [9], [10]	Measures body fluids such as sweat, tears, and saliva.	High distortion
Exhalation breath condensate [11]	Uses breath acetone as a biomarker for glucose metabolism.	Inaccurate & inefficient
Transdermal glucose extraction [12]	Uses reverse iontophoresis.	Inaccurate & inefficient

accuracy of the measured results. For example, the technique based on Raman spectroscopy is unstable due to the high interference between the light beam and the analyte [7], [8]. In addition, analysis of body fluids (e.g., sweat, tears, and saliva) could provide information about the glucose levels in the human body. However, it suffers from high distortion due to the deficient glucose levels in these fluids compared to that in blood [9], [10]. Similarly, the techniques utilizing the exhalation breath samples and reverse iontophoresis-based transdermal extraction are inefficient and inaccurate [11], [12].

Over the last two decades, there has been increased interest in wireless technologies and their related applications, including microwave/RF sensing of blood glucose concentrations. In addition, the desire to design medical diagnostic devices is motivated by the interaction of electromagnetic waves with physiological tissues that involve the study of dielectric property profiles of these tissues and their anomalies [13], [14], [15]. The electromagnetic wave behavior in a material is controlled by its dielectric properties, and hence these properties are considered one of the prime design considerations of the RF/microwave framework. The emergence of mobile wireless systems and then body-centric communications combined with the opportunity of using implantable devices for biological monitoring have motivated the study of the impact of electromagnetic waves on the human body [16].

Research on the dielectric properties of biological tissues has been extensively reported [17], [18], [19], [20]. A precise evaluation of the dielectric properties of the blood tissue is crucial to ensure successful microwave diagnostics and therapy, which relies mainly on the dielectric disparity between healthy and unhealthy tissues. Lately, researchers have been encouraged to examine the dielectric properties of blood glucose to pave the way for possible microwave-based noninvasive blood glucose-monitoring systems.

In [21], an empirical Cole–Cole formula was developed to characterize the dielectric properties of physiological tissues throughout a broad frequency spectrum. This formula is given as

$$\hat{\epsilon}(\omega) = \epsilon_\infty + \frac{\epsilon_s - \epsilon_\infty}{1 + (j\omega\tau)^{(1-\alpha)}} + \frac{\sigma_i}{j\omega\epsilon_0} \tag{1}$$

where ϵ_∞ is the relative permittivity at field frequencies, ϵ_s is the static permittivity, τ is the relaxation time for a dispersion region, α represents the broad distribution of the relaxation time constant, and σ_i is the ionic conductivity. The difference $\epsilon_s - \epsilon_\infty$ is denoted as $\Delta\epsilon$ and the effective permittivity $\hat{\epsilon}$ is a function of frequency.

The need for simple, accurate, fast, and noninvasive methods that can be utilized to monitor glucose levels in aqueous solutions has gained a lot of attention recently. Nevertheless, this was not possible until recent advances in microwave devices, microelectronics, telecommunications, and sensing systems [22], [23], [24].

Microwave-based methods for glucose detection are advantageous as they use a small volume of test samples and produce faster results, in contrast to traditional and laborious chemical techniques for glucose detection. Furthermore, these types of sensors have been successfully employed to detect glucose levels in aqueous solutions independent of the effects of interferents. The high sensitivity of the microwave sensors to the dielectric properties of the sample under test is due to changes in the resonant frequency and the magnitude and phase of the reflected signal off the sample under test. Therefore, they are frequently employed to detect glucose concentrations in an aqueous solution.

In [22], a metamaterial-based microfluidic sensor is proposed to detect glucose concentration in an aqueous solution. The proposed sensor utilizes an interdigital capacitor in the resonator that provides high sensitivity for testing dielectric liquids. On the other hand, Saleh et al. [23] reported an aqueous glucose detector based on a single asymmetric split ring resonator. The unique design confines the glucose solution within a specific area to maximize the field interactions between the electromagnetic waves and the subject under test. A Whispering Gallery Modes (WGM)-based glucose detector that comprises a dielectric disk resonator that couples to a dielectric image waveguide working in the mm-wave regime was recently proposed [24]. The operation of the sensor is based on the interaction between the aqueous glucose solution placed on the dielectric disk resonator and the WGM evanescent field.

In light of this progress toward delivering a portable noninvasive glucose monitoring system, this article proposes an end-to-end low-cost microwave-based sensing system capable of detecting glucose concentration through a noninvasive scheme. The contributions of this article are threefold: 1) propose two patch antennas to work as a biosensor; 2) propose a low-cost complete system solution, including the sensing mechanism and electronic circuits, that can be portable; 3) employ a new sensing mechanism based on the voltage measurements rather than the conventional microwave sensing methods based on the scattering parameters.

The article is structured as follows: the design of the proposed system, including the antenna and analog front-end design, is presented in Section II. Section III explains the experimental setup and methodology. In addition, the discussion and comparison with state-of-the-art techniques are presented. Finally, conclusions are drawn in Section IV.

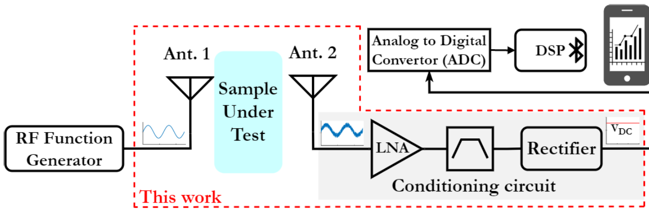

Fig. 1. Block diagram of the proposed glucose monitoring system.

II. Proposed System

The proposed system is depicted in Fig. 1. It comprises an RF source to transmit electromagnetic waves within the sample under test via the first antenna (Ant. 1). The RF signal is then received by another antenna (Ant. 2). The received signal is conditioned to be processed by a digital signal processing (DSP) unit (i.e., microcontroller). Finally, the information obtained by the DSP unit is wirelessly transmitted to a mobile device via Bluetooth in the form of a glucose reading. This section discusses the proposed system's design, including the design of the antenna, a biosensor, and an analog front-end circuit.

A. Antenna Design

The RF source used in this work is chosen to be a microstrip patch antenna due to the many advantages offered by this type of antenna [25], [26], [27], [28], [29], [30], [31]. These advantages include lightweight, small size, low cost, simple feeding structure, conformal nature, and can be shaped and placed on almost any surface. A microstrip antenna comprises a conductive pattern (also known as a radiating patch) printed on one side of a dielectric substrate and a ground plane on the opposite side of that substrate. The substrate material should be chosen carefully, as its height and dielectric constant significantly impact the antenna's performance and overall size. In addition, microstrip patch antennas can operate at multiple frequency bands (dual, triple) by controlling the shape and size of the radiating patch.

In this work and as shown in Fig. 2, a dual-band microstrip patch antenna is adopted as a sensing element. The commercial electromagnetic software CST Microwave Studio is employed to simulate the antenna and assess its performance. The antenna operates at resonance frequencies of 2.5 and 5.7 GHz. The antenna consists of a rectangular patch with five different slots on the patch and one large slot on the ground plane. The antenna is designed on an FR-4 substrate with a thickness of 1.6 mm and a dielectric constant of 4.3. The dimensions of the dual-band microstrip patch antenna are determined by the resonant frequency and the dielectric constant value. The antenna dimensions and the positioning of the slots are chosen such that the antenna operates at 2.5 and 5.7 GHz resonance frequencies.

Fig. 3 shows the simulated scattering parameters of the two antenna sensors when placed 7 cm apart facing each other, as seen in Fig. 2(d) and when there are no samples between the two antennas. The behaviors of the reflection coefficients (S_{11} and S_{22}) show that both antennas are well matched to the feeding microstrip line at 2.5 and 5.7 GHz. The -10 dB impedance bandwidth ranges from 5.6 to 6.7 GHz at the higher operating band. Fig. 4 shows the 3-D radiation pattern (directivity) at 5.7 GHz of the sensing antenna setup when Ant. 1 is excited, while Ant. 2 is terminated by a matched 50-Ω load. These far-field results show that the antenna radiation is directed from Ant. 1 to Ant. 2 with a maximum directivity of 4.51 dB. This directed radiated field will help detect the glucose in the water solution when placed midway between the two antennas.

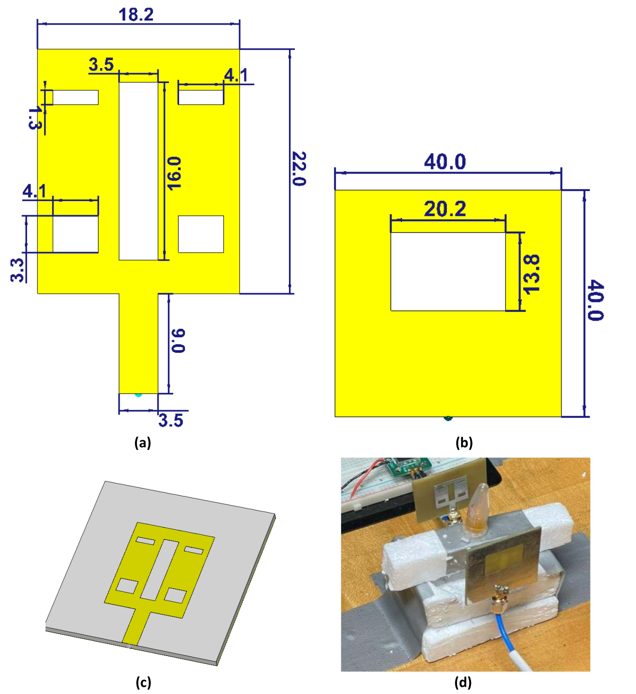

Fig. 2. (a) Top view of the dual-band patch antenna with five rectangular slots. (b) Back view showing the ground plane with a large rectangular slot. (c) Perspective view of the antenna. (d) Fabricated antenna prototype with a mock sample placed between the two sensing antennas (all dimensions are in mm).

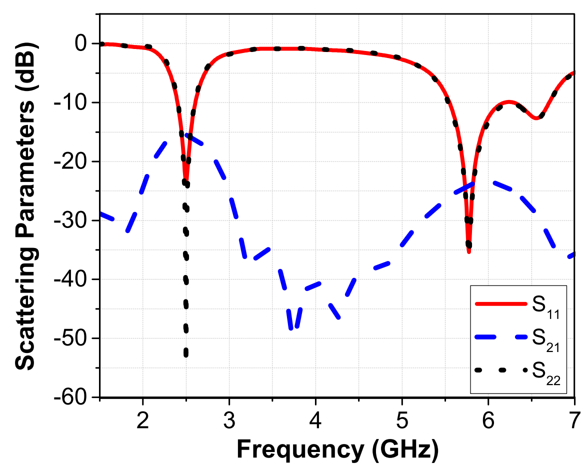

Fig. 3. Scattering parameters in dB of the two antenna sensors when placed 7 cm apart facing each other, as seen in Fig. 2(d) and when there are no samples between the two antennas.

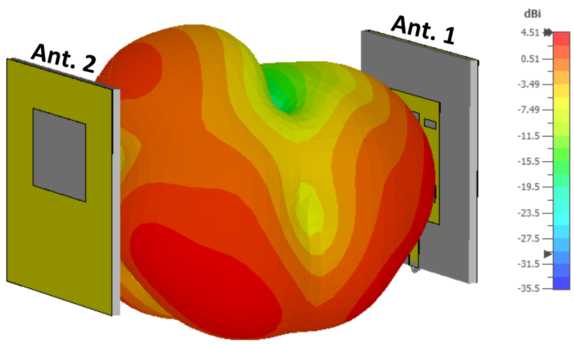

Fig. 4. Three-dimensional radiation pattern (directivity) at 5.7 GHz of the sensing antenna setup when antenna 1 (Ant. 1) is excited, while antenna 2 (Ant. 2) is terminated by a matched 50 Ω load.

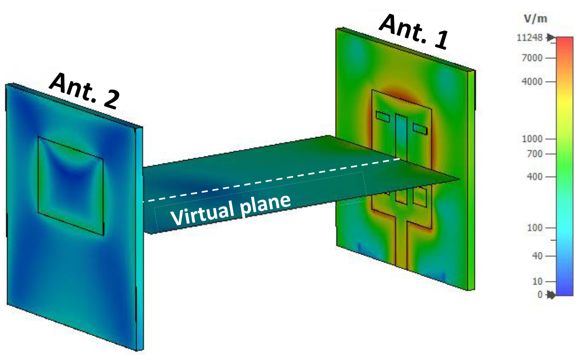

Fig. 5. Peak electric field (near-field) distribution at 5.7 GHz when Ant. 1 is excited, while Ant. 2 is terminated by a matched 50-Ω load. Adequate electric field intensity is observed between both antennas over the virtual plane shown.

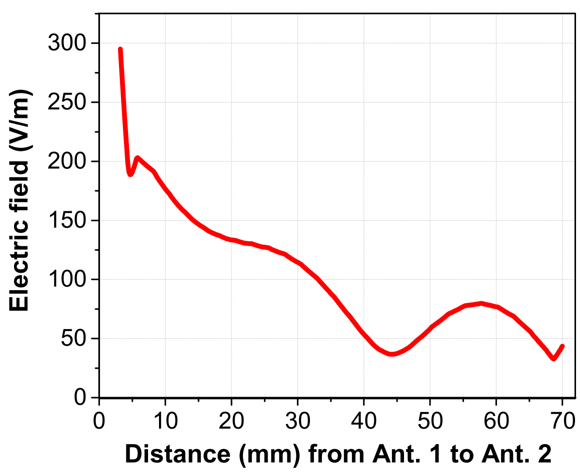

Fig. 6. Electric field in V/m calculated along the virtual dash-line between the two sensing antennas as seen in Fig. 5, starting from Ant. 1 to Ant. 2.

Fig. 5 illustrates the peak electric field (near-field) distribution at 5.7 GHz when Ant. 1 is excited while Ant. 2 is terminated by a matched 50-Ω load. Adequate electric field intensity is observed between both antennas over the virtual plane shown. Fig. 6 plots the electric field in V/m calculated along the virtual dash-line between the two antennas (see Fig. 5) starting from Ant. 1 to Ant. 2. The electric field decreases as we move away from the transmitting Ant. 1 toward the

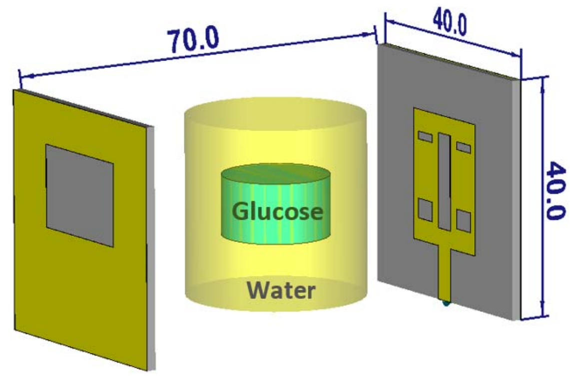

Fig. 7. Numerical simulation model of the water–glucose solution placed midway between the two sensing antennas (all dimensions are in mm).

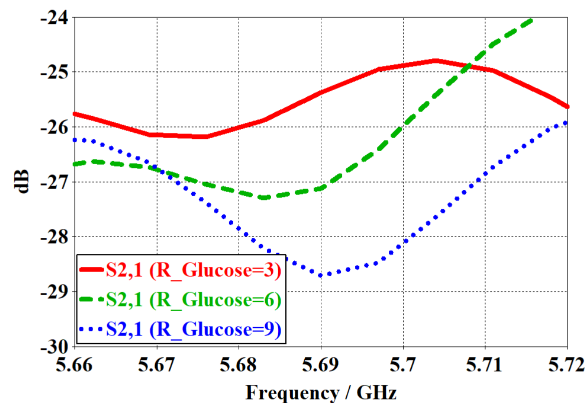

Fig. 8. Simulated transmission coefficient (S_{21}) in dB between the two antennas for different glucose levels in the water solution, "*R*_Glucose" is the radius (in mm) of the glucose sample as seen in Fig. 7.

receiving Ant. 2 with an adequate field value of about 85 V/m midway between both antennas (i.e., at distance 35 mm from Ant. 1) where the sample under test is to be placed.

To study the effect of increasing the glucose concentration in the water on the power transmitted between the two antennas, numerical simulations are conducted using the 3-D commercial electromagnetic software CST Studio Suite. Fig. 7 demonstrates the numerical setup model constructed in CST to mimic the empirical model seen in Fig. 10 (inset). Glucose–water solution is placed midway between the two sensing microstrip antennas operating at 5.7 GHz. The diameter of the cylindrical water volume is 30 mm with a height of 30 mm. To study the effect of increasing the glucose concentration in the water on the power transmitted between the two antennas, a piece of glucose is immersed in the water with a cylindrical shape of a constant height of 10 mm and varying radius of "*R*_Glucose". Note that the water volume is modeled in CST as a homogeneous material with a dielectric constant of 78.4 (distilled water) and a relative permeability of 1. While the glucose sample (see Fig. 7) is modeled, based on the results in [32] obtained at room temperature of 22 °C, as a glucose–water solution with a dielectric constant of 60 and relative permeability of 1. Fig. 8 shows the simulated transmission coefficient (S_{21}) in dB between the two antennas for different glucose levels in the water solution. Increasing the

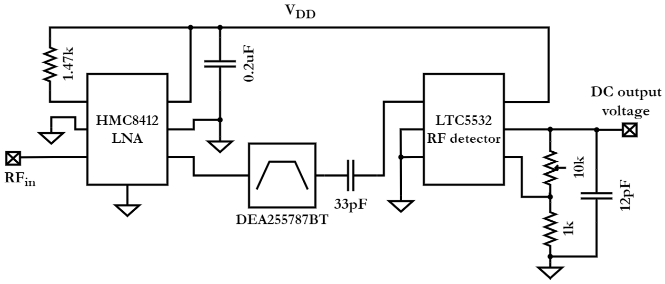

Fig. 9. Schematic of the conditioning circuit, including an LNA, BPF, and RF detector.

radius of the glucose sample decreases the power transmitted from the transmitting to the receiving antenna at 5.69 GHz, which matches the antenna operating resonance frequency, as expected.

B. Analog Readout Circuit

As discussed earlier, the overall system comprises transmitter and receiver sides as depicted in Fig. 1. The receiver side includes the conditioning circuit (i.e., analog readout circuit) that consists of a low-noise amplifier (LNA), a bandpass filter (BPF), and an RF detector. Fig. 9 shows the schematic of the conditioning circuit of the proposed system. The LNA is needed to provide good noise performance in addition to adequate amplification for the analog signal because the received RF signal by Ant. 2 is typically noisy, weak, and low in voltage amplitude (i.e., in the range of few hundreds μV to few mV). There are many circuit techniques to design efficient transistor-level LNA [33]. However, this article aims to provide a functioning glucose monitoring system holistically and to examine the practicality of the RF sensing mechanism. Hence, designing a specific LNA for this application is out of the scope of this article. Therefore, many off-the-shelf general-purpose LNAs have been investigated to be used in the proposed system. Details of the chosen LNA are presented in Section III.

For better signal conditioning, the filtering stage is implemented using a passive BPF that blocks undesirable low- and high-interference noises. The last stage of the conditioning circuit is the RF peak detector. It converts the RF ac signal power into a dc voltage level by envelope detection.

For the noise analysis of the conditioning circuit, the contributions of the LNA and BPF can be considered. The RF detector rectifies the RF signal, so its contribution to the noise can be ignored. Therefore, the noise factor of the receiver side of the system can be determined as follows:

$$F_R = F_{\text{LNA}} + \frac{F_{\text{BPF}} - 1}{A_{\text{LNA}}} \tag{2}$$

where F_R is the noise factor of the receiver side, F_{LNA} is the LNA noise figure, F_{BPF} is the BPF noise figure, and A_{LNA} is the LNA voltage gain. In addition to the suppression of the noise by the BPF, the noise figure of the BPF is down-scaled by the gain of the LNA as seen in (2). Hence, the noise of the conditioning circuit is mainly determined by the noise of the LNA. Section III provides details about the chosen components and related data to the electronic system's performance.

III. Experimental Results

The system is experimentally verified with the setup shown in Fig. 10. The conditioning circuit is implemented on an FR-4 printed circuit board (PCB) within an area of 4.32 × 1.78 cm, which is compatible with the Arduino nano board to be used for further signal processing. The proposed conditioning circuit comprises a GaAs-based LNA (HMC8412) from Analog Devices, which operates efficiently at 0.4–11 GHz and comes in Lead Frame Chip Scale Package (LFCSP), which is useful for system miniaturization. The LNA has a noise figure of 1.4 dB and an insertion loss of almost −0.3 dB, that is, 94% efficient in delivering the input power.

A multilayer BPF from TDK (DEA255787BT-2044A1) with a frequency range of 5.7–6 GHz is used. The BPF has about −1 dB insertion loss at 5.7 GHz. In addition, the RF detector is implemented using a high-precision wideband, 0.3–7 GHz, RF power detector (LTC5532) from Linear Technology. The RF function generator (N5183A MXG) is used to generate the signal to be transmitted through the antenna. This generator can generate 100 kHz–20 GHz signals with a power range of −20 dBm up to 15 dBm. The conditioning circuit consumes 306 mW at 5.1 V, supplied from an external power supply as shown in the experimental setup (Fig. 10).

A. Experimental Methodology

The experimental setup is to place the glucose–water solution sample between two antennas placed 7 cm apart, as seen in Fig. 10. Note that this is the smallest possible distance to accommodate the sample-under-test between both antennas. Hence, placing the two antennas as close as possible is desirable to increase the radiation emitted from Ant. 1 toward Ant. 2 that will be disturbed by the sample-under-test.

A high-frequency signal of 5.7 GHz is generated and transmitted using the first antenna through the sample. On the other side, the second antenna receives the signal with different power levels compared to the transmitted signals and feeds the received signals to the conditioning circuit. The received signal is amplified, filtered, and then rectified. The dc voltage at the output terminals of the conditioning circuit (i.e., output terminals of the RF power detector) is measured using a digital multimeter. The samples used for the tests are plastic cups filled with deionized water and different glucose concentrations in mg/dL. The glucose weight is measured using a sensitive balance (Mettler Teldo AL204). For this experiment, 25 testing glucose–water samples are used to cover the range from 0 to 5 g/dL with a step of 200 mg/dL of glucose concentration.

The objective of this experiment is to study the relationship between the dc output voltage, the glucose concentration, and the input power levels of the system. The first step is to measure the output voltage for the glucose-free sample (i.e., pure water only) for various power levels. Here, the input power is varied between 0 and 15 dBm. Then, all other glucose samples are tested using 15-dBm input power to show the trend

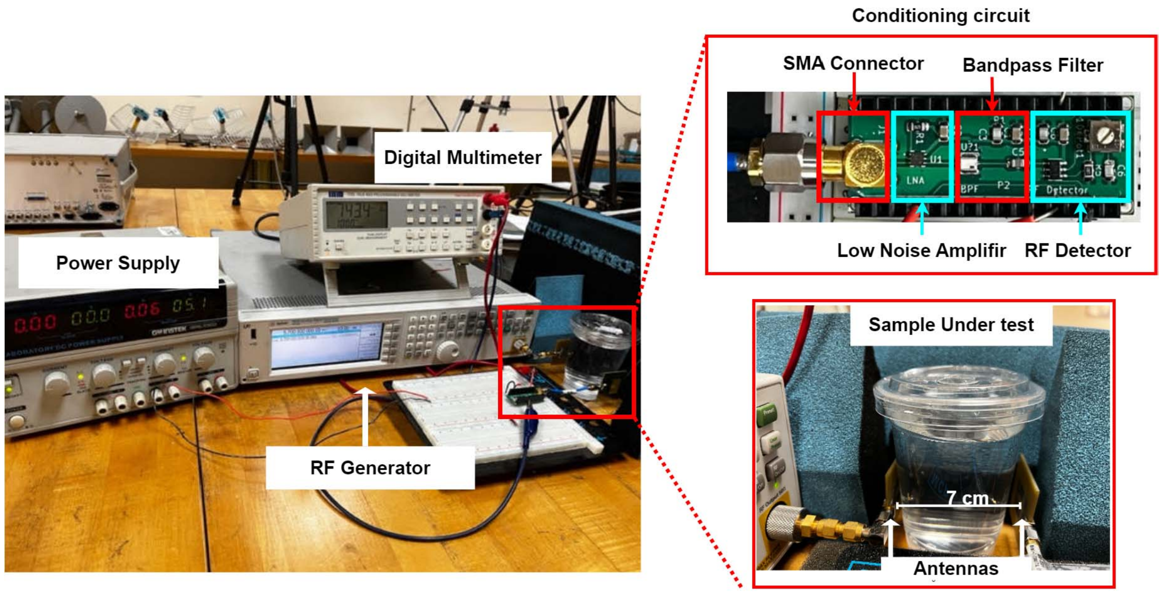

Fig. 10. Experimental setup of the proposed microwave-based noninvasive glucose monitoring system. The conditioning circuit is built on a standard PCB with an area of 1.78 × 4.32 cm^2.

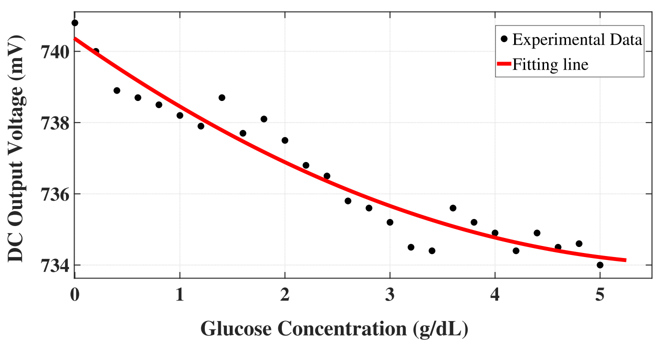

Fig. 11. Trend of the dc output voltage level compared to glucose concentration for P_{in} = 15 dBm. The experimental data represents the average dataset. The fitting line is generated using the curve-fitting tool.

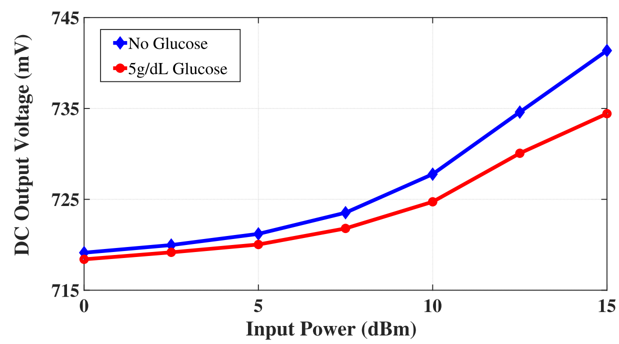

Fig. 12. DC output voltage versus the input power level using two extreme samples: glucose-free and 5 g/dL glucose.

in the output voltage compared to the glucose concentration. More glucose is added for each new test sample, and the output voltage is measured. Due to the sensitivity of the system, three different voltage measurements of each sample are taken and then averaged out.

B. Results Discussion

The dc output voltage versus glucose concentration is shown in Fig. 11. The experimental dataset comprises the average values of the measured output voltages for each sample. The output voltage decreases with increasing glucose concentration, which is expected. The system is tested using a wide range of glucose concentrations, that is, 0–5000 mg/dL. Hence, it is expected to have a nonlinear relation, as seen in Fig. 11, due to several factors, including aqueous solution characteristics, the container material, external RF noise, internal circuit noise, and other factors. For instance, viscosity increases nonlinearly with respect to the aqueous glucose solution [34]. Therefore, it is expected to have nonlinear dc voltage measurements. Nevertheless, the relation between the dc output voltage and glucose concentration follows a trend, as shown in Fig. 11. The MATLAB curve-fitting tool is used to show the correlation between the output voltage and the concentration. With second-degree polynomial fitting and 95% confidence bounds, the output voltage can be found as follows:

$$V_{\text{out}} = 0.18\ G^2 - 2.11\ G + 740.6 \tag{3}$$

where V_{out} is given in mV, and G is the glucose concentration level measured in g/dL.

In addition to the effect of the glucose concentration, this experiment also shows the effect of the input power on the sensitivity of the measured dc output voltage for different glucose–water samples. Fig. 12 illustrates the response of the dc output voltage to different power levels for two extreme cases (i.e., glucose-free and 5 g/dL glucose samples). As the input power increases, the measured dc output voltage increases, leaving more room to detect other glucose concentration levels. For low-input power levels, the difference between the two samples is very small, which makes it

TABLE II
PERFORMANCE OF THE PROPOSED GLUCOSE-SENSING SYSTEM COMPARED TO THE RECENT LITERATURE

Reference	Biosensor Technology	Operating Frequency	Glucose concentration (mg/dL)	Sensitivity (ΔX per 1mg/dL)	System Complexity
2021, [35]	Sub Terahertz Waveguide	110-170 GHz	70-145	ΔS_{21}= 0.13 dB	High
2013, [36]	Rectangular Cavity	1.91 GHz	0-2500*	ΔS_{21}=1.8e^{-5}dB, Δf_r= 0.015 kHz	Medium
2019, [37]	Millimeter-wave Horn Antenna	60-80 GHz	0-300	ΔS_{21}=2.3m dB, $\Delta\angle S_{21}$=0.0153°	High
2020, [38]	Split Ring Oscillator	2-3 GHz	0-400	ΔS_{21}=8e^{-5} dB	Medium
2015, [39]	Complementary Port Resonator	1.7 GHz	1000- 9000†	Δf_r= 21.1 kHz	Medium
2017, [40]	Single Port Resonator	4.8 GHz	0-1000	Δf_r= 14 kHz	Medium
2018, [41]	Ultra-wide Band Antenna	1-18 GHz	20-70†	Δf_r= 446 kHz‡	High
This Work	Patch Antennas	5.7 GHz	0-5000	ΔV_{DC}= 2.65 μV	Low

* Sucrose solution.
† Calculated. For example, 10 mg/mL is equivalent to 1000 mg/dL and 10% of glucose concentration is interpreted as 10 mg/dL.
‡ Calculated from (3) in [41] and considering a maximum change of 70% glucose concentration as reported in the same reference.

difficult for the conditioning circuit to distinguish between close glucose concentration levels. For example, the voltage range between two extreme samples, glucose-free and 5 g/dL glucose, is only 0.6 mV for $P_{\text{in}} = 0$ dBm. Consequently, the voltage sensitivity of the system degrades as the input power decreases. To elaborate, assume that the system will detect five glucose concentration levels, from 0 to 5 g/dL with a 1 g/dL step. For $P_{\text{in}} = 0$ dBm, the system has only 120 μV of voltage room for each concentration level in the best-case scenario. Therefore, at least a 16-bit ADC stage is required when a 5-V-voltage supply microcontroller is used. This stringent requirement increases the complexity and cost of the system. Therefore, the voltage range (i.e., the difference in the dc output voltage between two extreme samples, glucose-free, and 5-g/dL glucose concentration) is a useful measurement to optimize the performance and system complexity and identify the requirements of the electronic system. For this experiment, the voltage range for different power levels is illustrated in Fig. 13.

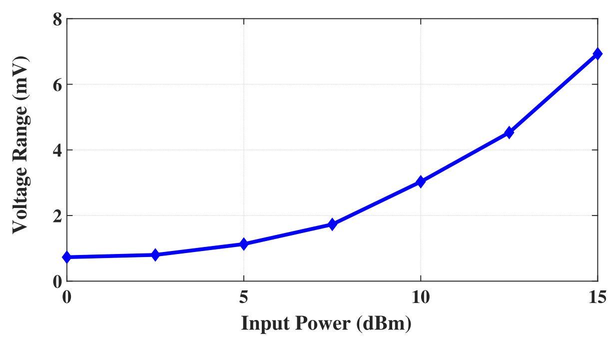

Fig. 13. Voltage range between two extreme samples, glucose-free, and 5 g/dL glucose concentration, versus different input power levels.

In this work, the voltage sensitivity of the system is interpreted as the amount of variation of the output variable (dc output voltage) with the variation of the input variable (glucose concentration) and can be quantified as follows:

$$\text{Sensitivity} = \frac{1}{n}\sum_{i=2}^{n}\left|\frac{V_{\text{dc}_i} - V_{\text{dc}_{i-1}}}{G_i - G_{i-1}}\right| \tag{4}$$

where n is the number of testing samples.

Table II shows a comparison between our proposed work and some of the state-of-the-art techniques reported in the literature. The experiments reported in [35], [37], [39], [40], and [38] are carried out using glucose–water samples and sucrose–water for [36], with an acceptable glucose concentration range. Meanwhile, Ebrahimi et al. [39] used a high glucose concentration range of 1000–9000 mg/dL which can be useful for food applications but not for human blood glucose, typically between 50 and 500 mg/dL. Conversely, a small glucose concentration range is used in [41] and [35]. For the proposed work, the experiments use 0–5000 mg/dL of glucose concentration range, which can be useful for medical and food applications. Although all references employ microwave-based techniques to detect glucose, the measured parameter is different. For example, the glucose level is detected using the magnitude of the transmission coefficient (S_{21}) [35], [36], [37], [38], the phase of S_{21} [37], and/or the change in resonance frequency (f_r) [39], [40], [41]. Nevertheless, all the work reported in Table II is based on using a Vector Network Analyzer, a very expensive and bulky equipment, to measure S_{21} or the resonant frequency. This significantly hinders the objective of providing a portable and low-cost glucose sensing system.

On the contrary, our proposed system is the first attempt to noninvasively detect glucose levels based on the voltage level of the received signal, which is useful for achieving a portable glucose monitoring system. The proposed system achieves a voltage sensitivity of 2.65 μV/mgdL^{-1} based on (4). It is worth mentioning that the system accuracy is vulnerable to several factors, such as the material of the container, the distance between the antennas, and any outer signal of the bandwidth of 5.7 GHz. As a result, several measures have been taken to design the experiment to ensure the best accuracy possible such as shortening the distance to the minimum, which is 7 cm and surrounding the sample with anechoic foam that absorbs any frequency higher than 125 Hz.

Regarding the system complexity shown in Table II, it considers the cost and portability of the system, which can be determined by the operating frequency and the availability of the electronic conditioning circuit in the proposed system. For high operating frequencies, off-the-shelf electronics become hard to find; hence, an application-specific integrated circuit (ASIC) is a must, which dramatically increases the cost of the system. To the best of the authors' knowledge, the proposed work is the first to provide a low-cost, noninvasive, and simple end-to-end system, which is missing in other reported designs.

Note that all the experimental work in this article was conducted at room temperature of 22 °C. We consider the study of the temperature dependence of glucose concentration in aqueous solutions as a potential future work of the current manuscript.

IV. Conclusion

This article addresses one of the most challenging scientific problems: noninvasive continuous glucose monitoring. The article proposed an end-to-end system that shows the practicality of glucose level detection using an RF antenna as a biosensor and in a noninvasive fashion. Moreover, the work presented in this article uses a new mechanism of sensing glucose via the voltage amplitude of the received signal. This way of sensing has not been reported in the literature. The experimental results show that there is a correlation between the glucose level and the dc output voltage. The system sensitivity is also studied for different input power levels. The proposed system achieved a voltage sensitivity of 2.65 μV/mgdL^{-1} using 15-dBm input power at 5.7-GHz frequency operation. The voltage sensitivity can be increased by providing more input power within an acceptable limit. The voltage-sensing mechanism in this work may ignite more ideas to simplify and design a low-cost portable noninvasive glucose monitoring system in the near future.

Acknowledgment

The authors thank Dr. Mohammad Al-Qahtani, Consultant in Pediatric Endocrinology and Diabetes at King Fahd Hospital of the University (KFHU), Khobar, Saudi Arabia, and an Associate Professor of Pediatrics at Imam Abdulrahman Bin Faisal University (IAU), Dammam, Saudi Arabia, for the fruitful and insightful discussions on blood glucose detection and continuous monitoring.

References

[1] P. Lakhera, S. Singh, R. Mehla, V. Chaudhary, P. Kumar, and S. Kumar, "Boronic acid decorated graphene nano flakes for glucose sensing in diabetes: A DFT prediction," *IEEE Sensors J.*, vol. 22, no. 8, pp. 7572–7579, Apr. 2022.

[2] Z. Ye, J. Wang, H. Hua, X. Zhou, and Q. Li, "Precise detection and quantitative prediction of blood glucose level with an electronic nose system," *IEEE Sensors J.*, vol. 22, no. 13, pp. 12452–12459, Jul. 2022.

[3] D. Bruen, C. Delaney, L. Florea, and D. Diamond, "Glucose sensing for diabetes monitoring: Recent developments," *Sensors*, vol. 17, no. 8, pp. 336–343, 2017. [Online]. Available: https://www.mdpi.com/1424-8220/17/8/1866

[4] M. Iyer, "Compact antenna with artificial magnetic conductor for noninvasive continuous blood glucose monitoring," M.S. thesis, Dept. Elect. Eng., Rochester Inst. Technol., Rochester, NY, USA, 2018.

[5] ISO. *In Vitro Diagnostic Test Systems Requirements for Blood-Glucose Monitoring Systems for Self-Testing in Managing Diabetes Mellitus*. Accessed: Jul. 2022. [Online]. Available: https://www.iso.org/standard/54976.html

[6] Continuous Glucose Monitoring System. *FreeStyle Libre System*. Accessed: Jul. 1, 2022. [Online]. Available: https://www.freestyle.abbott/us-en/products/freestyle-libre-3.html

[7] A. J. Berger, T.-W. Koo, I. Itzkan, G. Horowitz, and M. S. Feld, "Multicomponent blood analysis by near-infrared Raman spectroscopy," *Appl. Opt.*, vol. 38, no. 13, pp. 2916–2926, May 1999. [Online]. Available: http://opg.optica.org/ao/abstract.cfm?URI=ao-38-13-2916

[8] J. W. Kang et al., "Direct observation of glucose fingerprint using in vivo Raman spectroscopy," *Sci. Adv.*, vol. 6, no. 4, Jan. 2020, Art. no. eaay5206, doi: 10.1126/sciadv.aay5206.

[9] C. Liao, M. Zhang, M. Y. Yao, T. Hua, L. Li, and F. Yan, "Flexible organic electronics in biology: Materials and devices," *Adv. Mater.*, vol. 27, no. 46, pp. 7493–7527, Dec. 2015, doi: 10.1002/adma.201402625.

[10] P. Makaram, D. Owens, and J. Aceros, "Trends in nanomaterial-based non-invasive diabetes sensing technologies," *Diagnostics*, vol. 4, no. 2, pp. 27–46, Apr. 2014. [Online]. Available: https://www.mdpi.com/2075-4418/4/2/27

[11] C. N. Tassopoulos, D. Barnett, and T. R. Fraser, "Breath-acetone and blood-sugar measurements in diabetes," *Lancet*, vol. 293, pp. 1282–1286, Jun. 1969.

[12] D. C. Klonoff, "Continuous glucose monitoring: Roadmap for 21st century diabetes therapy," *Diabetes Care*, vol. 28, no. 5, pp. 1231–1239, 2005, doi: 10.2337/diacare.28.5.1231.

[13] Y. Gao, M. T. Ghasr, M. Nacy, and R. Zoughi, "Towards accurate and wideband in vivo measurement of skin dielectric properties," *IEEE Trans. Instrum. Meas.*, vol. 68, no. 2, pp. 512–524, Feb. 2019.

[14] O. Güren, M. Çayören, L. T. Ergene, and I. Akduman, "Surface impedance based microwave imaging method for breast cancer screening: Contrast-enhanced scenario," *Phys. Med. Biol.*, vol. 59, no. 19, p. 5725, 2014.

[15] R. W. Paglione, "Coaxial applicator for microwave hyperthermia," U.S. Patent 4 204 549 May 27, 1980.

[16] Y. Hao, A. Brizzi, R. Foster, M. Munoz, A. Pellegrini, and T. Yilmaz, "Antennas and propagation for body-centric wireless communications: Current status, applications and future trend," in *Proc. IEEE Int. Workshop Electromagn., Appl. Student Innov. Competition*, Aug. 2012, pp. 1–2.

[17] C. Gabriel, S. Gabriel, and E. Corthout, "The dielectric properties of biological tissues: I. Literature survey," *Phys. Med. Biol.*, vol. 41, no. 11, pp. 2231–2249, Nov. 1996, doi: 10.1088/0031-9155/41/11/001.

[18] S. Gabriel, R. W. Lau, and C. Gabriel, "The dielectric properties of biological tissues: II. Measurements in the frequency range 10 Hz to 20 GHz," *Phys. Med. Biol.*, vol. 41, no. 11, pp. 2251–2269, Nov. 1996, doi: 10.1088/0031-9155/41/11/002.

[19] S. Gabriel, R. W. Lau, and C. Gabriel, "The dielectric properties of biological tissues: III. Parametric models for the dielectric spectrum of tissues," *Phys. Med. Biol.*, vol. 41, no. 11, p. 2271, Nov. 1996.

[20] M. Lazebnik et al., "A large-scale study of the ultrawideband microwave dielectric properties of normal, benign and malignant breast tissues obtained from cancer surgeries," *Phys. Med. Bio.*, vol. 52, no. 20, p. 6093, Oct. 2007.

[21] K. S. Cole and R. H. Cole, "Dispersion and absorption in dielectrics I. Alternating current characteristics," *J. Chem. Phys.*, vol. 9, no. 4, pp. 341–351, 1941.

[22] G. Govind and M. J. Akhtar, "Metamaterial-inspired microwave microfluidic sensor for glucose monitoring in aqueous solutions," *IEEE Sensors J.*, vol. 19, no. 24, pp. 11900–11907, Dec. 2019.

[23] G. Saleh, I. S. Ateeq, and I. Al-Naib, "Glucose level sensing using single asymmetric split ring resonator," *Sensors*, vol. 21, no. 9, p. 2945, Apr. 2021. [Online]. Available: https://www.mdpi.com/1424-8220/21/9/2945

[24] A. E. Omer, S. Gigoyan, G. Shaker, and S. Safavi-Naeini, "WGM-based sensing of characterized Glucose-aqueous solutions at mm-waves," *IEEE Access*, vol. 8, pp. 38809–38825, 2020.

[25] B. Wang and Y. Lo, "Microstrip antennas for dual-frequency operation," *IEEE Trans. Antennas Propag.*, vol. AP-32, no. 9, pp. 938–943, Sep. 1984.

[26] S. Ghosh and B. K. Sarkar, "Design of microstrip crossed monopole antenna for ultra wideband communication microstrip crossed monopole for ultra wideband communication," in *Proc. Annu. IEEE India Conf. (INDICON)*, Dec. 2012, pp. 499–502.

[27] Z. Zhou, Z. Wei, Z. Tang, and Y. Yin, "Design and analysis of a wideband multiple-microstrip dipole antenna with high isolation," *IEEE Antennas Wireless Propag. Lett.*, vol. 18, pp. 722–726, 2019.

[28] Y. Kimura, K. Furukawa, S. Saito, Y. Kimura, and T. Fukunaga, "Design of wideband multi-ring microstrip antennas fed by an L-probe for single-band and dual-band operations," in *Proc. IEEE Int. Symp. Antennas Propag. North Amer. Radio Sci. Meeting*, Jul. 2020, pp. 541–542.

[29] Y. Suo, W. Li, and H. Wang, "A dual-band notched ultra wideband microstrip antenna," in *Proc. IEEE Int. Symp. Antennas Propag. USNC/URSI Nat. Radio Sci. Meeting*, Jul. 2017, pp. 1787–1788.

[30] R. H. Thaher and Z. S. Jamil, "Design of dual band microstrip antenna for Wi-Fi and WiMax applications," *Telkomnika*, vol. 16, no. 6, pp. 2864–2870, 2018.

[31] A. Chaabane, F. Djahli, H. Attia, L. M. Abdelghani, and T. A. Denidni, "Wideband and high-gain EBG resonator antenna based on dual layer PRS," *Microw. Opt. Technol. Lett.*, vol. 59, no. 1, pp. 98–101, Jan. 2017.

[32] X. Liao, V. G. S. Raghavan, V. Meda, and V. A. Yaylayan, "Dielectric properties of supersaturated α-D-glucose aqueous solutions at 2450 MHz," *J. Microw. Power Electromagn. Energy*, vol. 36, no. 3, pp. 131–138, Jan. 2001.

[33] B. Razavi, "Design of millimeter-wave CMOS radios: A tutorial," *IEEE Trans. Circuits Syst. I, Reg. Papers*, vol. 56, no. 1, pp. 4–16, Jan. 2009.

[34] V. R. N. Telis, J. Telis-Romero, H. B. Mazzotti, and A. L. Gabas, "Viscosity of aqueous carbohydrate solutions at different temperatures and concentrations," *Int. J. Food Properties*, vol. 10, no. 1, pp. 185–195, Jan. 2007, doi: 10.1080/10942910600673636.

[35] P. Kaurav, S. K. Koul, and A. Basu, "Non-invasive glucose measurement using sub-terahertz sensor, time domain processing, and neural network," *IEEE Sensors J.*, vol. 21, no. 18, pp. 20002–20009, Sep. 2021.

[36] G. Gennarelli, S. Romeo, M. R. Scarfi, and F. Soldovieri, "A microwave resonant sensor for concentration measurements of liquid solutions," *IEEE Sensors J.*, vol. 13, no. 5, pp. 1857–1864, May 2013.

[37] S. Hu, S. Nagae, and A. Hirose, "Millimeter-wave adaptive glucose concentration estimation with complex-valued neural networks," *IEEE Trans. Biomed. Eng.*, vol. 66, no. 7, pp. 2065–2071, Nov. 2019.

[38] C. Jang, J. K. Park, H. J. Lee, G. H. Yun, and J. G. Yook, "Non-invasive fluidic glucose detection based on dual microwave complementary split ring resonators with a switching circuit for environmental effect elimination," *IEEE Sensors J.*, vol. 20, no. 15, pp. 8520–8527, Apr. 2020.

[39] A. Ebrahimi, W. Withayachumnankul, S. F. Al-Sarawi, and D. Abbott, "Microwave microfluidic sensor for determination of glucose concentration in water," in *Proc. IEEE 15th Medit. Microw. Symp. (MMS)*, Nov. 2015, pp. 1–3.

[40] V. Turgul and I. Kale, "Simulating the effects of skin thickness and fingerprints to highlight problems with non-invasive RF blood glucose sensing from fingertips," *IEEE Sensors J.*, vol. 17, no. 22, pp. 7553–7560, Nov. 2017.

[41] A. K. Jha et al., "Broadband wireless sensing system for non-invasive testing of biological samples," *IEEE Trans. Emerg. Sel. Topics Circuits Syst.*, vol. 8, no. 2, pp. 251–259, Jun. 2018.

Yaqub Mahnashi (Senior Member, IEEE) received the B.Sc. and M.Sc. degrees in electrical engineering from the King Fahd University of Petroleum and Minerals (KFUPM), Dhahran, Saudi Arabia, in 2008 and 2012, respectively, and the Ph.D. degree in electrical engineering from Michigan State University, East Lansing, MI, USA, in 2018.

From 2008 to 2009, he was an Instrumentation and Control Design Engineer with Saudi Basic Industrial Corporation (SABIC), Jubail, Saudi Arabia. Since 2009, he has been with KFUPM, where he is currently an Assistant Professor with the Department of Electrical Engineering. He is also a member of the Communication Systems and Sensing Research Center, KFUPM. His current research interests include switched-capacitor circuits, IC power converters, filter design, and low-power circuits for biomedical and energy-harvesting applications.

Dr. Mahnashi received the SABIC Scholarship in 2007; the Discovery Scholarship from the King Abdullah University of Science and Technology (KAUST) in 2009; and the Excellence in Teaching Award from the College of Engineering and Physics, KFUPM, in 2022.

Khurram Karim Qureshi (Senior Member, IEEE) received the B.Sc. (Hons.) degree in electrical engineering from the University of Engineering and Technology (UET), Lahore, Pakistan, in 1999, and the Ph.D. degree in electrical engineering from The Hong Kong Polytechnic University, Hong Kong, in 2006.

He is the Founder of the Optical Communications and Sensors Laboratory (OCSL) and a Full Professor with the Electrical Engineering Department, King Fahd University of Petroleum and Minerals (KFUPM), Dhahran, Saudi Arabia. He is also an affiliate of the Communication Systems and Sensing Research Center, KFUPM. He has published more than 100 journal and conference papers and holds five U.S. patents issued to his credit. His research interests include optical communications, optical signal processing, fiber and quantum dash lasers, optical sensors, and miniaturized antennas.

Abdullah A. Al-Shehri is currently pursuing the B.Sc. degree in electrical engineering with the Department of Electrical Engineering and the Center of Communication Systems and Sensing, King Fahd University of Petroleum and Minerals (KFUPM), Dhahran, Saudi Arabia.

He led the Senior Design Project Team to work on designing, prototyping, and testing a noninvasive glucose monitoring system in the Fall of 2021. He is skilled in circuit design, printed circuit board (PCB) design, and hardware testing. He is also working with Saudi Aramco, as a Trainee Project Engineer, in 2022.

Hussein Attia (Member, IEEE) received the B.Sc. (Hons.) degree in electronics and communication engineering from Zagazig University, Zagazig, Egypt, in 1999, and the Ph.D. degree in electrical and computer engineering from the University of Waterloo, Waterloo, ON, Canada, in 2011.

He worked as a Research Engineer with the Coding and Signal Transmission Laboratory, University of Waterloo, from March 2011 to July 2013. He was granted a Postdoctoral Fellowship at Concordia University, Montreal, QC, Canada, from August 2014 to July 2015. Also, he was a Visiting Scholar with the University of Quebec (INRS), Quebec, QC, Canada, from August 2015 to December 2015 and from June 2017 to August 2017. He is currently an Associate Professor with the King Fahd University of Petroleum and Minerals (KFUPM), Dhahran, Saudi Arabia. He has published more than 80 journal and conference papers. His research interests include millimeter-wave and wide-band antennas, EM sensors for biomedical applications, analytical techniques for electromagnetic modeling, and engineered magnetic metamaterials.

Dr. Attia received the University of Waterloo Graduate Scholarship for Excellence in Research and Coursework in 2009, during his Ph.D. program. He was the Finalist in the Student Paper Competition of the 2011 IEEE Antennas and Propagation Society (AP-S) International Symposium on Antennas and Propagation.